

Information processing based on an external-cavity semiconductor laser with optical feedback-phase modulation

Kazutaka Kanno^{†,1}, Chihiro Sugano^{‡,2}, Kousuke Takano^{‡,3}, Atsushi Uchida^{‡,4}, and Masatoshi Bunsen^{†,5}

[†]Department of Electronics Engineering and Computer Science, Fukuoka University,
8–19–1 Nanakuma, Johnan-ku, Fukuoka, Japan

[‡]Department of Information and Computer Sciences, Saitama University,
255 Shimo-Okubo, Sakura-ku, Saitama City, Saitama, 338–8570, Japan

Email: kkanno@fukuoka-u.ac.jp¹, c.sugano.912@ms.saitama-u.ac.jp², k.takano.983@ms.saitama-u.ac.jp³,
auchida@mail.saitama-u.ac.jp⁴, bunsen@fukuoka-u.ac.jp⁵

Abstract—Reservoir computing (RC) based on a semiconductor laser with time-delayed optical feedback is numerically demonstrated. RC is a machine learning paradigm based on information processing in the human brain. In our system, input information is injected into the laser via the phase of its optical feedback and any other laser is not used for information input. We demonstrated a chaotic time-series prediction by our RC system. We investigated the dependence of the prediction error on the feedback strength, the laser’s injection current, and a node interval by which a feedback loop is temporally divided for considering virtual nodes. The numerical simulation showed that the prediction error reduces as the injection current is increased when the feedback strength and the node interval are properly adjusted. Because signal to noise ratio is improved at a large value of the injection current.

1. Introduction

Reservoir Computing (RC) is machine learning paradigm [1]. RC can process empirical data and is inspired by the way that the brain processes information. Conventional RC systems utilize a neural network which has a large number of nodes. Recently, delay-based RC, where a time-delayed dynamical system is used instead of a neural network, has been proposed [2]. In that scheme, nodes are considered by temporally dividing feedback delay with a small interval θ , which is called a node interval. When an input signal is injected into the time-delayed dynamical system, the system produces a transient response and virtual node states can be obtained from the response. The output of RC is given by a weighed linear combination of the virtual node states, where the weights are decided in a training procedure.

Also in optics, delay-based RC has been studied, where the reservoir is an external cavity semiconductor laser [3]. The laser system consists of a semiconductor laser and a time-delayed optical feedback loop. A semiconductor laser can response to inputs with a high oscillation frequency (exceeding to a few GHz), which results in high speed information processing. In that optical RC scheme, input sig-

nals are injected into the reservoir via optical injection from another semiconductor laser. This input scheme requires injection locking of the reservoir to the injected light [4]. This requirement restricts the magnitude of the injection current because a large value of the injection current in the reservoir may prevent injection locking. In fact, the injection current has been adjusted to the threshold one in some literatures [3–5]. The output power of a laser is low on the condition of the threshold current and the signal to noise ratio cannot be improved.

Recently, RC based on an erbium doped microchip laser with input signals injected via modulating the intensity of optical feedback has been proposed [6]. This scheme does not require another laser for information input and the signal to noise ratio can be improved as the injection current is increased. In this study, we numerically demonstrate RC based on an external cavity semiconductor laser with an input signal injected via modulating the phase of optical feedback. We modulate only the phase of the optical feedback for information input and the optical intensity of the laser is not modulated directly. However, the laser produces complex responses in the intensity dynamics. We demonstrate a chaotic time-series prediction by our RC system and evaluate the prediction performance.

2. RC based on a semiconductor laser

Our RC scheme based on an external cavity semiconductor laser is addressed in this section. The schematic diagram of our RC system is shown in Fig. 1. The RC system consists of three parts; an input layer, a reservoir, and an output layer. The reservoir is an external cavity semiconductor laser with feedback phase modulation. In the input and output layers, preprocessing for input signals and post-processing for the output of the reservoir are performed, respectively. In the following subsections, we explain the delay-based RC method and show our numerical model.

2.1. Delay-based RC scheme

Delay-based RC, where a reservoir is a single nonlinear node with delayed feedback, has been recently intro-

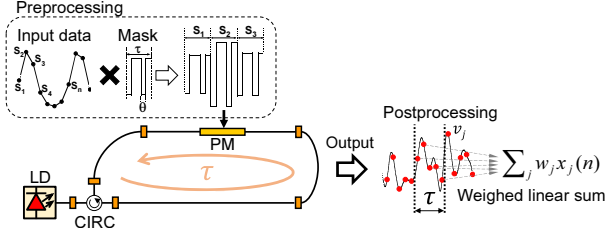


Figure 1: Schematic diagram of our RC system based on an external cavity semiconductor laser. LD is the laser diode. CIRC is the optical circulator and realizes optical feedback. PM is the phase modulator and the phase of optical feedback is modulated by the PM. The delay time of optical feedback is represented by τ .

duced [2]. In that scheme, a delayed nonlinear node emulates a network of a large number of connected nodes. Nodes are virtually implemented within a delay line by time-multiplexing. These nodes are called virtual nodes. Virtual nodes connect with neighboring nodes and have self feedback. Therefore, the configuration of the virtual network is a ring topology. Our reservoir has optical feedback with delay time τ and virtual nodes are implemented by temporally dividing τ with a small time interval θ , which is called node interval. The number of virtual nodes N is given by $N = \tau/\theta$. The states of virtual nodes are extracted from the temporal intensity waveform of the laser output.

In the input layer, preprocessing for input data is performed. We consider time discrete data s_n ($n = 1, 2, \dots$ is the discrete time) as an input. Each input data is injected into the reservoir for the duration of τ since virtual nodes are implemented in a delay line. Then, a mask signal $m(t)$ is multiplied with input data to keep the laser transient state. The mask acts as input weights to virtual nodes. To implement the same input weights for all of each input data, the period of the mask is equal to the delay time τ . The mask used in this work is a piecewise step function with the step interval θ and the value of the mask is randomly chosen from the set $\{-1, -0.3, 0.3, 1\}$. The input signal multiplied with the mask is given by the following equation:

$$s(t) = \gamma m(t) s_n \quad ((n-1)\tau \leq t < n\tau), \quad (1)$$

where γ is the scaling factor which scales the amplitude of $s(t)$. We set to $\gamma = 0.5$.

A weighed linear combination of virtual node states is calculated in the output layer and the calculation result is the output of RC. The output $y(n)$ for the n -th input data is given by the following equation,

$$y(n) = \sum_{j=1}^N w_j x_j(n), \quad (2)$$

where x_j is the node state and w_j is the weight for the j -th node state. The node state x_j is extracted from the temporal output of the laser. The weight w_j is trained by minimizing

the mean-square error between the target function $\bar{y}(n)$ and the RC output $y(n)$ as follows,

$$\frac{1}{N_{tr}} \sum_{j=1}^{N_{tr}} (y(n) - \bar{y}(n))^2 \rightarrow \min, \quad (3)$$

where N_{tr} is the number of input data for training.

2.2. Numerical model for an external cavity semiconductor laser

The reservoir is an external cavity semiconductor laser with feedback phase modulation. The dynamics of such model is described by the Lang-Kobayashi equations [7]. The equations are given by the following:

$$\frac{dE(t)}{dt} = \frac{1 + i\alpha}{2} \left\{ \frac{G_N(N(t) - N_0)}{1 + \epsilon|E(t)|^2} - \frac{1}{\tau_p} \right\} E(t) + \kappa E(t - \tau) \exp\{i[s(t) - \omega\tau]\} + \xi(t), \quad (4)$$

$$\frac{dN(t)}{dt} = J - \frac{N(t)}{\tau_s} - G_N(N(t) - N_0)|E(t)|^2, \quad (5)$$

where E is the slowly varying complex electric field amplitude and N is the carrier density. G_N is the gain coefficient, N_0 is the carrier density at transparency, α is the linewidth enhancement factor, τ_p and τ_s are the photon and carrier lifetimes, and J is the injection current of the laser. The injection current J is given by the product of the threshold current J_{th} and j . ω is the angular optical frequency of the laser and given by $\omega = 2\pi/\lambda$, where $\lambda = 1547$ nm is the optical wavelength of the laser. These parameter values are set to the same as in [8].

The second term in the right hand side of Eq. (4) represents optical feedback. κ and τ in the term are the feedback strength and the feedback delay time, respectively. $s(t) - \omega\tau$ represents the phase shift due to phase modulation and delay. The delay time τ is related to the number of nodes N and the node interval θ . N is given by $\tau = N\theta$. In our RC system, the number of nodes is two hundreds and the node interval is varied.

The last term $\xi(t)$ in the right hand side of Eq. (4) represents the effect of spontaneous emission noise. $\xi_{1,2}(t)$ is complex number and degenerates the performance of RC.

3. Chaotic time-series prediction by RC

To evaluate the performance of our RC scheme, we use the Santa-Fe time-series prediction task [9]. The aim of the task is to perform single-point-prediction of chaotic time-series. The time-series is generated from a far-infrared laser. We use the first 3,000 points in the time-series for training and the last 1,000 points for testing.

The performance of the prediction task is quantitatively evaluated by using the normalized mean-square error (NMSE) as follows,

$$NMSE = \frac{1}{N_{te}} \frac{\sum_{j=1}^{N_{te}} (y(n) - \bar{y}(n))^2}{\sigma^2}, \quad (6)$$

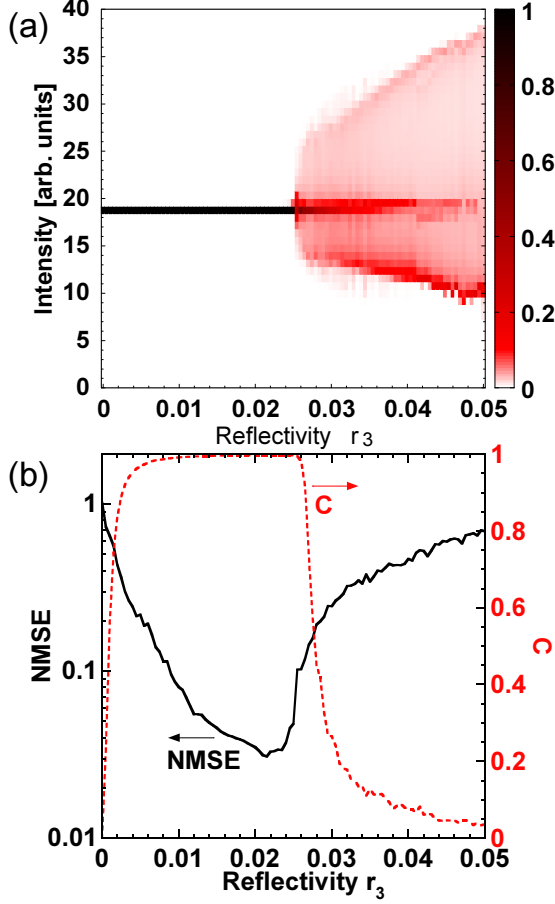


Figure 2: (a) Bifurcation diagram of the laser dynamics as a function of the reflectivity r_3 . The color map represents the probability of the laser intensity. (b) Dependence of the NMSE and C on r_3 .

where N_{te} is the number of input data in the test procedure. σ is the standard deviation of $\bar{y}(n)$. The NMSE represents the difference between the target $\bar{y}(n)$ and the output $y(n)$ of RC, and the NMSE close to zero indicates a low prediction error.

Firstly, we relate the prediction performance to the temporal dynamics of the reservoir without input signals. We vary the reflectivity r_3 for changing the temporal dynamics. Figure 2(a) shows the bifurcation diagram as a function of r_3 . The diagram is constructed from the probability distribution of the laser intensity $I(t) = |E(t)|^2$. The range of the intensity (the vertical axis) from 0 to 40 is divided into 50 bins and the probability for each bins is represented by color. The black color means that the probability is equal to one and the dynamics of the laser is a temporally steady state. The intensity distribution is extended when the reflectivity exceeds $r_3 = 0.0250$, where the transition of dynamical state occurs. The dynamics of the laser at $r_3 = 0.0260$ is quasi-periodic. It is expected that the transition of dynamical state affects the consistency property of the reservoir. Consistency is an ability that dynamical

systems driven by a repeated signal generates reproducible responses [10]. Reproducible results are necessary for RC. We investigate the consistency property of our RC system and relate the temporal dynamics of the laser.

A quantitative measure of consistency is given by the cross-correlation coefficient among two response signals. The response signals are the output of the reservoir which is repeatedly driven by the same input signal, which is a masked input signal for the chaotic time-series prediction task. The cross-correlation coefficient is calculated by using the following equation;

$$C = \frac{\langle (I_1(t) - \bar{I}_1)(I_2(t) - \bar{I}_2) \rangle}{\sigma_1 \sigma_2}, \quad (7)$$

where $I_i(t)$ is the optical intensity response of the laser when the i -th input is injected into the reservoir. \bar{I}_i is the average intensity and σ_i is the standard deviation of $I_i(t)$. $\langle \cdot \rangle$ denotes time averaging. C nearly equal one indicates that consistency is achieved.

Figure 2(b) shows the dependence of the NMSE (the black solid curve) and C (the red dashed curve) on the feedback strength. C is nearly equal to zero at $\kappa = 0$, where the reservoir has no input signal since the input signal is injected into the reservoir via modulating the feedback phase. As the feedback strength is increased, C increases and approaches one. Since the input signal is injected via the feedback phase, increasing the feedback strength enhances modulation strength by the input signal. The enhancement of the modulation strength can improve signal-to-noise ratio. Therefore, the consistency property C is improved. However, the largest value of C is obtained at $r_3 = 0.0220$ and shows a large decrease at $r > 0.0250$, where the laser changes its dynamical state from a temporally steady state as shown in Fig. 2(a).

The dependence of the NMSE is shown in the black solid curve of Figs 2(b). The NMSE decreases as increasing r_3 and the lowest value of the NMSE is obtained at $r_3 = 0.0215$. Comparing the result with the bifurcation diagram shown in Fig. 2(a), it is found that the lowest value of the NMSE is produced at r_3 just near to the dynamical transition point ($r_3 = 0.0250$). However, the NMSE increases as increasing r_3 in $r_3 > 0.0250$. The dependence of the NMSE is also related to the consistency property. It is found that the lowest value of the NMSE is given at r_3 where a large value of the consistency property is obtained. Therefore, r_3 should be set to a value a little smaller than a dynamical transition point.

Next, we investigate the dependence of RC performance on the injection current j . When the injection current is varied, the reflectivity r_3 and the node interval θ need to be properly adjusted to enhance RC performance. Figures 3(a) and 3(b) show the map of the NMSE on the parameter space of r_3 and θ at $j = 1.50$ and 3.00 , respectively. In Fig. 3(a), the lowest value of the NMSE is obtained at $r_3 = 0.013$ and $\theta = 0.14$ ns. In Fig. 3(b), on the other hand, the lowest value is obtained at $r_3 = 0.045$ and $\theta = 0.04$ ns.

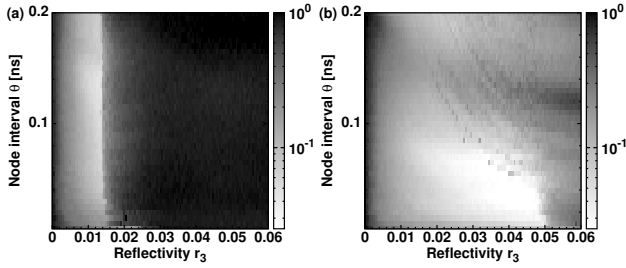


Figure 3: Two-dimensional map of the NMSE as a function of the reflectivity r_3 and the node interval θ . The color map shows the value of the NMSE. The injection current j for (a) and (b) is 1.5 and 3.0, respectively.

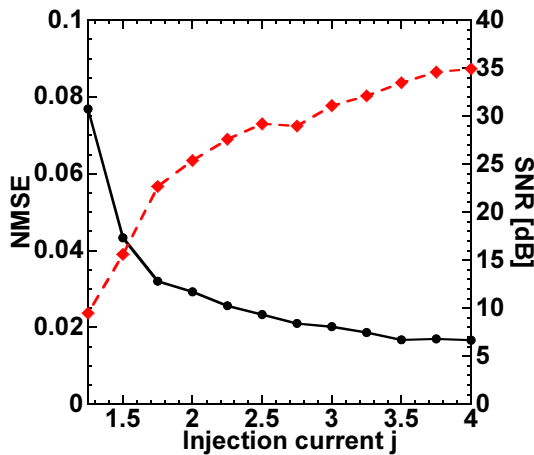


Figure 4: NMSE (the black solid curve) and SNR (the red dashed curve) as a function of the injection current j . The reflectivity r_3 and the node interval θ are properly adjusted at an each value of j .

These results indicate that a large value of r_3 and a small interval of θ are required for high performance at a large value of the injection current. It has been known that a larger value of r_3 is required for arising dynamical transition at a larger value of j [11]. Since the prediction performance is improved at r_3 just near to a dynamical transition point, a large value of r_3 is required for high performance at a larger value of j . On the other hand, the node interval is related to a relaxation oscillation frequency. It has been known that the node interval corresponding to one-fifth of the inverse of the relaxation oscillation frequency is suited for RC [3]. The relaxation oscillation frequency of a semiconductor laser is enhanced as increasing j . Therefore, a small value of the node interval is required at a large value of the injection current.

Figure 4 shows the dependence of the NMSE on the injection current j when the reflectivity and the node interval are properly adjusted at an each value of j . We also show the dependence of the signal to noise ratio (SNR). The SNR is defined as $10 \log_{10}(v_s/v_n)$, where v_s and v_n are the standard deviations of the response signal of the reservoir

and the temporal output of the reservoir without an input signal, respectively. We find that the NMSE decreases as the injection current j is increased. One of the reasons why the NMSE decreases is the improvement of the SNR, which is shown in the red dashed curve. It is also important to be able to utilize a large value of the reflectivity when the injection current is large. Because a large value of the reflectivity can lead to the enhancement of memory capacity in the reservoir.

4. Conclusion

We numerically demonstrated RC based on an external cavity semiconductor laser. In our RC scheme, the input signal is injected into the reservoir via the phase of optical feedback. The performance of RC was quantitatively evaluated using the chaotic time-series prediction task. We investigate the dependence of the prediction accuracy on the injection current. The prediction accuracy is improved as the injection current is increased when the reflectivity and the node interval are properly adjusted at an each value of the injection current.

References

- [1] H. Jaeger and H. Haas, *Science*, vol. 304, no. 5667, pp. 78–80 (2004).
- [2] L. Appeltant, M.C. Soriano, G.V. derSande, J. Danckert, S. Massar, J. Dambre, B. Schrauwen, C.R. Mirasso, and I. Fischer, *Nat. Commun.*, vol. 2, pp. 468–1–6 (2011).
- [3] D. Brunner, M.C. Soriano, C.R. Mirasso, and I. Fischer, *Nat. Commun.*, vol. 4, pp. 1364–1–7 (2013).
- [4] J. Bueno, D. Brunner, M.C. Soriano, and I. Fischer, *Opt. Express*, vol. 25, no. 3, pp. 2401–2412 (2017).
- [5] K. Hicke, M. Escalona-Moran, D. Brunner, M.C. Soriano, I. Fischer, and C.R. Mirasso, *Selected Topics in Quantum Electronics, IEEE Journal of*, vol. 19, no. 4, pp. 1501610–1501610 (2013).
- [6] R.M. Nguimdo, E. Lacot, O. Jacquin, O. Hugon, G.V. derSande, and H.G. deChatellus, *Opt. Lett.*, vol. 42, no. 3, pp. 375–378 (2017).
- [7] R. Lang and K. Kobayashi, *IEEE Journal of Quantum Electronics*, vol. 16, pp. 347–355 (1980).
- [8] K. Kanno and A. Uchida, *Phys. Rev. E*, vol. 86, pp. 066202–1–9 (2012).
- [9] A.S. Weigend and N.A. Gershenfeld, *IEEE International Conference on Neural Networks*, vol.3, pp. 1786–1793 (1993).
- [10] A. Uchida, R. McAllister, and R. Roy, *Phys. Rev. Lett.*, vol. 93, pp. 244102 (2004).
- [11] A. Uchida, *Optical Communication with Chaotic Lasers, Applications of Nonlinear Dynamics and Synchronization*, Wiley-VCH, Weinheim, 2012.